DINAME 2015 - Proceedings of the XVII International Symposium on Dynamic Problems of Mechanics
V. Steffen, Jr; D.A. Rade; W.M. Bessa (Editors), ABCM, Natal, RN, Brazil, February 22-27, 2015

The Impact of Kinematic and Actuation Redundancy on the Energy Efficiency of Planar Parallel Kinematic Machines

Andrés Gómez Ruiz, João Vitor de Carvalho Fontes and Maíra Martins da Silva

[1] Department of Mechanical Engineering, São Carlos School of Engineering, University of São Paulo, Av. Trabalhador Sancarlense, 400. CEP: 13566590, São Carlos SP, Brazil

Abstract: Higher energy efficiency can be reached by the use of parallel manipulators in industry. Nevertheless, serial manipulators are the frequent choice. Among others, a huge limitation of parallel manipulators is the amount of singularities in their workspace. Several studies have shown that both actuator and kinematic redundancies promote a significant reduction in the singularities and homogenization on the actuation forces. In this paper, an energy-efficient trajectory planning strategy is employed to evaluate three planar parallel kinematic manipulators: the 3RRR, the 4RRR and the (P)RRR+2RRR. The 3RRR presents no redundancy, while the 4RRR and the (P)RRR+2RRR presents actuator and kinematic redundancies, respectively. Two important results can be found: (i) the optimal energy-efficient trajectories are dependent on the manipulator architecture and (ii) redundant parallel manipulators can be more energy efficient.

Keywords: energy efficiency, trajectory planning, parallel kinematic machines, redundancy

NOMENCLATURE

A = location of the active joints
B = location of the passive joints of the end-effector
c = center of the end-effector
E = energy
f = force
l = longitude of one branch
M = location of the branch passive joints
m = number of joints
n = time samples
P = power
v = linear velocity
x = horizontal coordinate
y = vertical coordinate
J = jacobian matrix
p = inertia force and moment matrix

Greek Symbols
θ = Active Joint Angle
β = Passive Joint Angle
ϕ = Orientation angle
δ = Displacement of the linear actuator
τ = torque
$\boldsymbol{\tau}$ = driving torques matrix
ω = angular velocity
$\boldsymbol{\Omega}$ = partial velocities and angular velocities matrix

INTRODUCTION

Nowadays, energy consumption is a big concern in the international community. According to the U.S. Energy Information Administration (*eia*), the industrial sector consumed 52% of the global delivered energy in 2010, and its energy consumption grows by an average of 1.4 percent per year from 2010 to 2040. The European Union (EU) has established a goal for reduce its energy consumption by 20% (compared with projected levels) by 2020.

In view of the facts, the development of energy efficient systems is a must. In the work, (Li and Bone, 2001), is proved that over a range of conditions, the average energy usage of the parallel manipulators was determined to be 26% of the serial manipulators. In this respect, a slight improve in the energy consumption on favor of parallel manipulators in pick-and-place industrial robots application is shown in Pellicciari et al. (2013).

The last statistics and examples are the motivation for investigate parallel kinematic machines (PKMs). The main limitation of PKMs is the presence of singularities. Singularity avoidance has been present in the *state of the art* of PKMs during last years. Some approaches for this purpose are centered in the path and trajectory planning, (Kim et al. 2004 and Mayorga and Chandama, (2006)). The presence of singularities in the *3RRR* is first introduced by Gosselin and Angeles (1990). Addition of redundancy seems to be a good solution to the problem of singularities in PKMs. Actuation redundancy consist in the addition of one or more chains. In the case of the *3RRR*, the addition of a new chain will originate the *4RRR*, Wu et al.(2010) suggest that the use of kinematic redundancy minimizes the presence of singularities. On the other hand, kinematic redundancy consist in the addition of an active joint in one of the kinematic chains, the addition of a prismatic joint to the *3RRR* origins the *(P)RRR+2RRR*. Kotlarsky et al. (2009) prove that this kind of redundancy applied to the *3RRR* allows to avoid singular configurations. The three PKMs under study are show in Fig. 1.

The objective of this text is to show the effects of the addition of actuation and kinematic redundancy in the energy efficiency of PKMs, for this purpose, a simulation procedure for analyze the energy performance over a chosen trajectory is presented.

The numerical methodology employed to model the studied manipulators is briefly described in Section 2 and 3. The methodological approach to evaluate the energy consumption is presented in Section 4. Numerical results are presented

in Section 5. In Section 6, final considerations and conclusions are described.

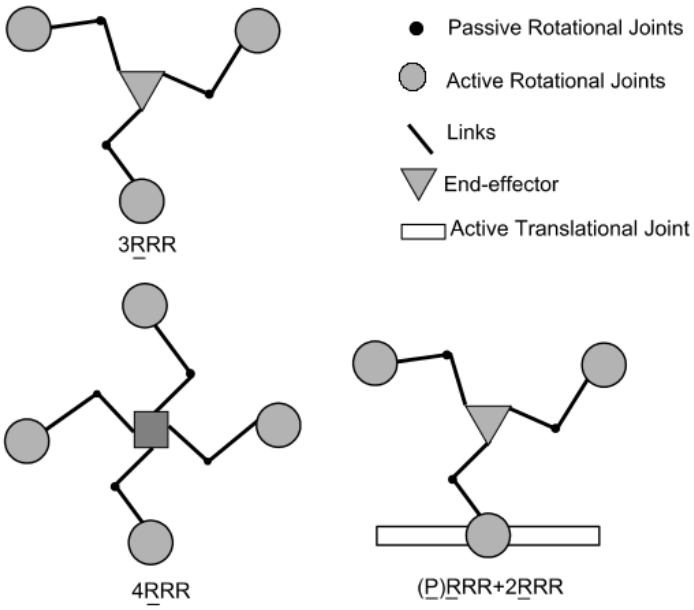

Figure 1 – *3RRR*: Planar parallel manipulator, *4RRR* and *(P)RRR+2RRR*: Redundantly actuated planar parallel manipulators.

INVERSE KINEMATICS

3RRR and *4RRR*.

In order to compute the angles θ_i, performed by the active rotational joints, during a given trajectory, the same reasoning described by Wu et al. (2010) is used. Figure 2 shows a single link, l_1 and l_2 are the lengths of the two branches of each link. The coordinate frame $(\overline{x}, \overline{y})$ has its origin in the point c, and is rotated ϕ degrees referential to the (x, y) frame.

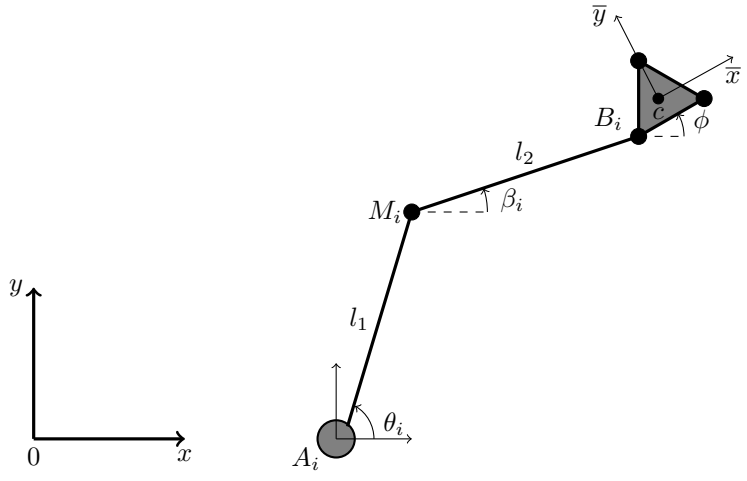

Figure 2 – Geometrical picture of one link.

The vector $\overrightarrow{M_iB_i}$ can be expressed as:

$$\overrightarrow{M_iB_i} = \begin{bmatrix} x_c \\ y_c \end{bmatrix} + \begin{bmatrix} \cos\phi & -\sin\phi \\ \sin\phi & \cos\phi \end{bmatrix} \begin{bmatrix} \overline{x}_{BCi} \\ \overline{y}_{BCi} \end{bmatrix} - \begin{bmatrix} x_{Ai} \\ y_{Ai} \end{bmatrix} - \begin{bmatrix} \cos\theta_i \\ \sin\theta_i \end{bmatrix} l_1 \tag{1}$$

With this we can define two quantities:

$$\begin{bmatrix} a_i \\ b_i \end{bmatrix} = \begin{bmatrix} x_c \\ y_c \end{bmatrix} + \begin{bmatrix} \cos\phi & -\sin\phi \\ \sin\phi & \cos\phi \end{bmatrix} \begin{bmatrix} \overline{x}_{BCi} \\ \overline{y}_{BCi} \end{bmatrix} - \begin{bmatrix} x_{Ai} \\ y_{Ai} \end{bmatrix} \tag{2}$$

It is clear from Fig. 2 that $||\overrightarrow{M_iB_i}|| = l_2$, therefore:

$$a_i^2 + b_i^2 + l_1^2 - l_2^2 - 2a_i l_1 \cos\theta_i - 2b_i l_1 \sin\theta_i = 0 \tag{3}$$

Last equation can be expressed as:

$$e_{i3} + e_{i2}\cos\theta_i + e_{i1}\sin\theta_i = 0 \tag{4}$$

Providing the expression to compute the angles θ_i:

$$\theta_i = 2\tan^{-1}\left(\frac{-e_{i1} \pm \sqrt{e_{i1}^2 + e_{i2}^2 - e_{i3}^2}}{e_{i3}^2 - e_{i2}^2}\right) \tag{5}$$

Equation (1) can be wrote as:

$$\begin{bmatrix} a_i - l_1\cos\theta_i \\ b_i - l_1\sin\theta_i \end{bmatrix} = l_2 \begin{bmatrix} \cos\beta_i \\ \sin\beta_i \end{bmatrix} \tag{6}$$

Therefore, angles β_i can be computed as:

$$\beta_i = \tan^{-1}\left(\frac{b_i - l_1\sin\theta_i}{a_i - l_1\cos\theta_i}\right) \tag{7}$$

(P)RRR+2RRR.

For the case of the (P)RRR+2RRR a linear guide is added. In this way, one of the rotary joints located at points A_i is not fixed and can move linearly along the guide, therefore, a new variable δ, that describes this linear displacement must be added to Eq. (1), as Fontes and da Silva (2014) describes.

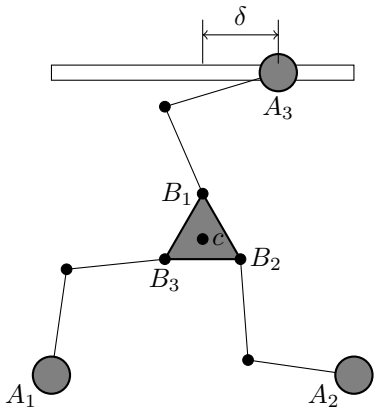

Figure 3 – Illustration of the linear displacement δ in the (P)RRR+2RRR.

In order to simplify the inverse kinematics, the chosen active joint is allowed to displace only in the x direction, see Fig. 3. Therefore, new quantities $a_1, a_2, a_3, b_1, b_2, b_3$ must be defined:

$$\begin{bmatrix} a_1 \\ b_1 \end{bmatrix} = \begin{bmatrix} x_c \\ y_c \end{bmatrix} + \begin{bmatrix} \cos\phi & -\sin\phi \\ \sin\phi & \cos\phi \end{bmatrix} \begin{bmatrix} \overline{x}_{BC1} \\ \overline{y}_{BC1} \end{bmatrix} - \begin{bmatrix} x_{A1} \\ y_{A1} \end{bmatrix} \tag{8}$$

$$\begin{bmatrix} a_2 \\ b_2 \end{bmatrix} = \begin{bmatrix} x_c \\ y_c \end{bmatrix} + \begin{bmatrix} \cos\phi & -\sin\phi \\ \sin\phi & \cos\phi \end{bmatrix} \begin{bmatrix} \overline{x}_{BC2} \\ \overline{y}_{BC2} \end{bmatrix} - \begin{bmatrix} x_{A2} \\ y_{A2} \end{bmatrix} \tag{9}$$

$$\begin{bmatrix} a_3 \\ b_3 \end{bmatrix} = \begin{bmatrix} x_c \\ y_c \end{bmatrix} + \begin{bmatrix} \cos\phi & -\sin\phi \\ \sin\phi & \cos\phi \end{bmatrix} \begin{bmatrix} \overline{x}_{BC3} \\ \overline{y}_{BC3} \end{bmatrix} - \begin{bmatrix} x_{A3} \\ y_{A3} \end{bmatrix} - \begin{bmatrix} \delta \\ 0 \end{bmatrix} \tag{10}$$

Substituting the quantities a_i and b_i defined in Eq. (3-7), with those defined in Eq. (8-10), allows to compute the angles θ_i and β_i for the (P)RRR+2RRR manipulator.

JACOBIAN MATRIX AND INVERSE DYNAMICS

Next section shows a briefly description of the methodology used to find the dynamic parameters of the system, details can be found in Wu et al. (2010).
Jacobian matrix J, relates the velocities of the end-effector with the velocities of the actuators:

$$\mathbf{A}\begin{bmatrix}\dot{x}\\ \dot{y}\\ \dot{\phi}\end{bmatrix} = \mathbf{B}\begin{bmatrix}\dot{\theta}_1\\ \dot{\theta}_2\\ \dot{\theta}_3\\ \dot{\delta}\end{bmatrix} \tag{11}$$

Where Jacobian matrix is expressed as:

$$\mathbf{J} = \mathbf{A}^{-1}\mathbf{B} \tag{12}$$

When the Jacobian matrix is computed, it is possible to find the velocities and the accelerations of the actuators. Inertia forces and moments are obtained with the Newton-Euler formulation. Afterwards, the driving torques, denoted as $\boldsymbol{\tau}$, can be found using the virtual work principle:

$$\boldsymbol{\tau J^T} - \boldsymbol{\Omega p} = \mathbf{0} \tag{13}$$

$\boldsymbol{\Omega}$ represents the partial linear and angular velocities matrix, $\boldsymbol{p}$ represents the inertia force and moment matrix.

ENERGY MODEL

As described by Bi and Wang (2012), once the driving torques and forces are obtained, the power consumption P is obtained as:

$$P(t) = \sum_{j=1}^{m_l} f_j(t)v_j(t) + \sum_{i=1}^{m_r} \tau_i(t)\omega_i(t) \tag{14}$$

In last equation, $f_j(t)$ is the driving force of a linear actuator; $\tau_i(t)$ is the driving torque of a rotary actuator; $v_j(t)$ is the velocity of the linear actuator; $\omega_i(t)$ is the angular velocity of the rotary actuator; m_l and m_r are the number of linear and rotary actuators respectively.
Energy can be obtained from Eq. (14) as:

$$E = \int \left[\sum_{j=1}^{m_l} f_j(t)v_j(t) + \sum_{i=1}^{m_r} \tau_i(t)\omega_i(t)\right] dt \tag{15}$$

In this paper, energy will be evaluated in several points of a given trajectory along a discrete interval of time, thus, energy will be expressed for each time sample n:

$$E(n) = \left[\sum_{j=1}^{m_l} f_j(n)v_j(n) + \sum_{i=1}^{m_r} \tau_i(n)\omega_i(n)\right] \Delta n \tag{16}$$

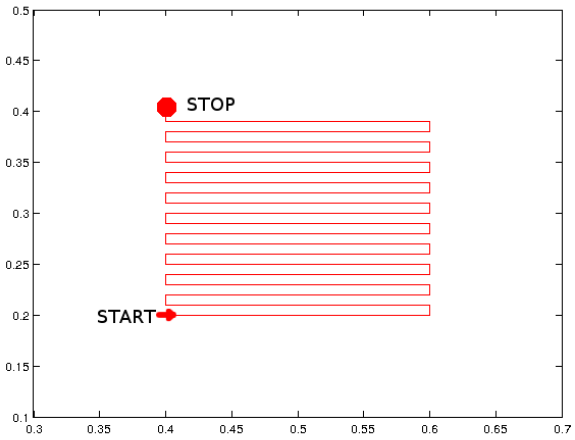

Figure 4 – Illustrative description of the used path.

SIMULATION PROCEDURE

On the present work, MATLAB routines are used in order to simulate the movements performed by the three PKMs under study; *3RRR*, *4RRR* and *(P)RRR+2RRR*. Each manipulator's end-effector will perform the same trajectory. An illustration of the performed path is described in Fig. 4. The end-effector is located originally in the position START, from this position performs a straight line to the right of 0.2 m, then, a slight movement in the vertical direction is performed, subsequently, the end-effectors moves to the left, again in a straight line of 0.2 m, another slight movement in the vertical direction is performed then. This path is executed several times until reach the position STOP, which is located 0.2 m above the START position. As have been mentioned, Fig. 4 is merely an illustration, for the simulated results the distances between the horizontal red lines in Fig. 4 are 0.001 m length. For this reason, the performed path gets the appearance of a squared area to the human eye, those areas are shown in red color on Fig. 5. The limits of the workspace are defined by the blue line in Fig. 5. The red squared areas that defines the performed path are centered in the center of the workspace for both manipulators, *3RRR* and *4RRR*, therefore a fair comparative can be established. The workspace for the (P)RRR+2RRR is assumed to be the same as the *3RRR*.

As described above, the path performed by the manipulator's end-effector consist in the reiteration of four consecutive movements: *(i)* a horizontal straight line of 0.2 m from the left to the right, *(ii)* a vertical straight line of 0.001 m from the bottom to the top, *(iii)* a horizontal straight line of 0.2 m from the right to the left, *(iiii)* the same moment described by *(ii)* is performed again. The trajectories just mentioned are described by fifth order polynomials. Figure 6 shows the curves for position, velocity and acceleration of the described paths.

For simulation purposes, data about inertia moments, masses, lengths and end-effectors architecture has been specified in Tab. 1.

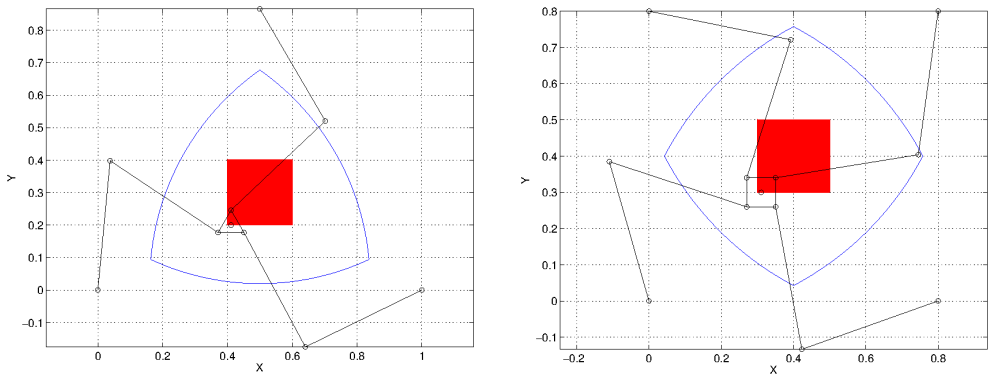

Figure 5 – Area described by the chosen trajectory for, a) *3RRR* and (P)RRR+2RRR, b) *4RRR*.

Table 1 – Manipulators specifications.

Property	Value
Links length (m)	0.4
Links 1 mass (Kg)	7.0067
Links 2 mass (Kg)	1.1735
Links 1 Inertial moment (Kg·m^2)	0.0779
Links 2 Inertial moment (Kg·m^2)	0.0677
End-effector mass (Kg·m^2)	0.1421
End-effector Inertial moment (Kg·m^2)	0.000563

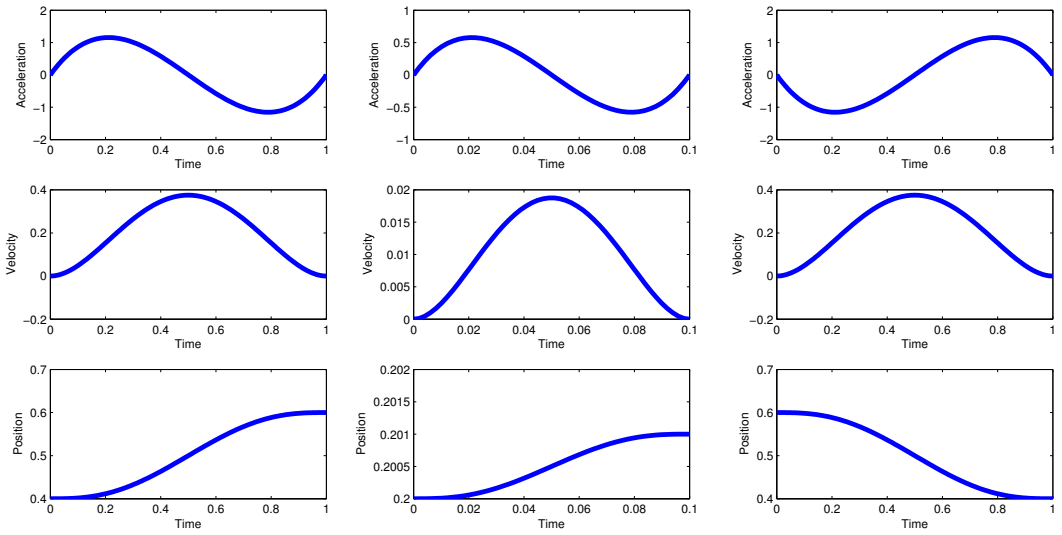

Figure 6 – Accleration, velocity and positions profiles for the the movements: a)*(i)* b)*(ii)* and c)*(iii)*.

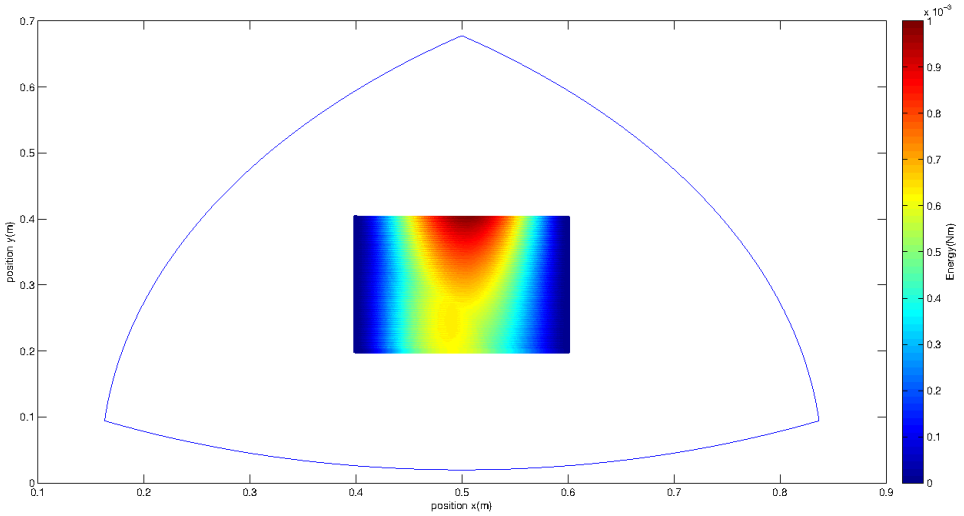

Figure 7 – 3RRR Energy distribution with ϕ=0 degrees.

RESULTS

In this section comparative results of the three PKMs under study are shown. Equation (16) has been used in order to get a value of the energy for each point of the trajectory. As an example of the obtained results, energy distribution for the *3$\underline{R}$RR* can be seen in Fig. 7. For space saving, just the square area where the energy is evaluated will be shown in the next figures. The observation of the energy distribution for the three PKMs, shows the importance of the choice of orientation angle ϕ, and the dependency of the position in the y axis with the energy consumption. Some of the orientations angles are not achievable due to contact between links. In order to avoid those collisions, the links can be built at different levels of altitude. On this sense, the *4$\underline{R}$RR* is advantageous in front of the other two manipulators, because it presents a square architecture end-effector in stead of triangular, which allows to reach bigger orientation angles.

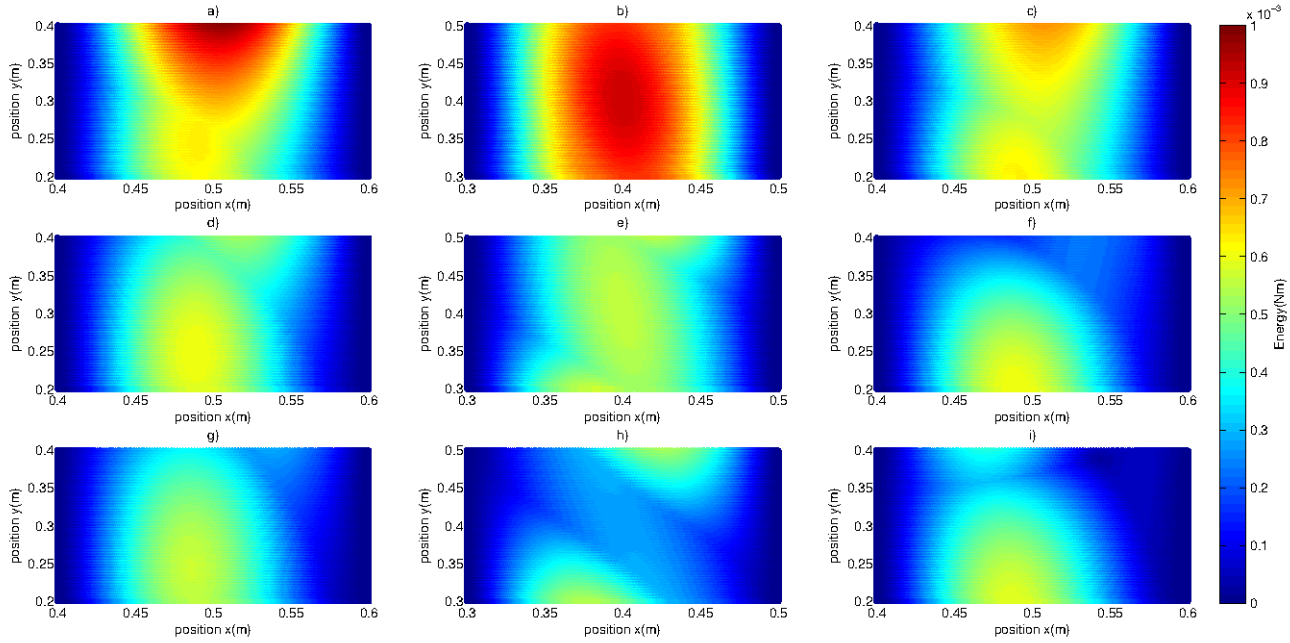

Figure 8 – Energy distribution for: a) *3RRR* with ϕ=0, b) *4RRR* with ϕ=0, c) (P)RRR+2RRR with ϕ=0 and δ=0.15, d) *3RRR* with ϕ=30, e) *4RRR* with ϕ=30, f) (P)RRR+2RRR with ϕ=30 and δ=0.15, g) *3RRR* with ϕ=60, h) *4RRR* with ϕ=60, i) (P)RRR+2RRR with ϕ=60 and δ=0.15.

Energy distribution for the three PKMs under three different values for the angle ϕ is evaluated in Fig. 8. Generally it has been observed that energy consumption decreases as orientation angle ϕ increases.

In Fig. 9, each data color represents a value of ϕ. For orientation angles between 45 and 90 degrees, a higher energy efficiency of the *4RRR* in front of the *3RRR* is noticed when the end-effector is located in middle position of the y axis. Angles in the range of 45 to 90 degrees are more easily attached by the *4RRR*, due to its own architecture.

As has been mentioned, the parallel manipulator (P)RRR+2RRR posses an additional variable δ. The presence this variable, allows the (P)RRR+2RRR manipulator to adopt an infinite number of configurations for an unique position of the end-effector. This fact leads to a problem of optimization for choose a value of δ. On this respect, several texts makes difference between *on line* and *off line* optimization. During the *on line* optimization the linear actuator and the end-effector are moving at the same time, benefits of this kind of optimization has been shown by Fontes and da Silva (2014). In the *off line* optimization the linear actuator moves to a previously chosen position and remains fixed, afterwards, the end-effector performs its movement, Kotlarski et al. (2008) propose an *off-line* based optimization to increase the end-effector pose accuracy.

In this text, only the *off line* optimization is considered. It is assumed that the necessary energy to move the linear actuator and hold it in the desired position is small in comparison with the energy consumed by the manipulator in the hole trajectory, therefore it is not considered.

A discrete interval of values of δ is used to evaluate the energy efficiency. Figure 10 presents comparative results of the manipulator (P)RRR+2RRR under different configurations, each data color represents a value for δ. Figure 10.c ($\phi = 45$), represents lowest energy consumption along the top position of the y axis when $\delta = 0.2$ (green), and $\delta = 0.3$ (red).

As a final result the Tab. 2 presents the absolute values of the energy consumed during the hole trajectory, most of the conditions used during this work has been reflected in this table. For the evaluated conditions the (P)RRR+2RRR is the best energy efficient, despite of this, perhaps a real (P)RRR+2RRR can not reach big orientation angles as 90 degrees, even so, it is clearly the best in the average. A real *4RRR* is able to reach higher orientation angles than the other two manipulators, therefore, the *4RRR* can gain more profit of the orientation angle.

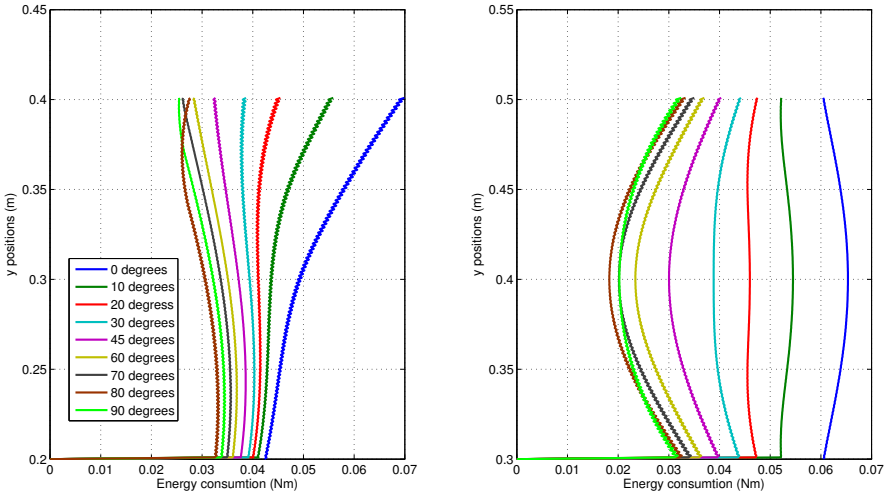

a) **b)**

Figure 9 – Variation of the energy consumption with the y axis position for: a) *3RRR*, b) *4RRR*

Table 2 – Total Energy consumption (Nm).

	(P)RRR+2RRR						*3RRR*	*4RRR*
	δ=-0.1	δ=-0.2	δ=-0.3	δ=0.1	δ=0.2	δ=0.3		
ϕ=0	10.3105	8.6276	5.9071	9.6167	8.6980	8.6800	10.5084	12.8310
ϕ=10	9.1813	7.7688	5.3671	8.1458	7.2275	7.3036	9.1563	10.7623
ϕ=20	8.5647	7.3536	5.1643	7.3184	6.4242	6.6023	8.3892	9.2790
ϕ=30	8.1663	7.1022	5.0673	6.8276	5.9913	6.2892	7.9016	8.1413
ϕ=45	7.6930	6.7985	4.9506	6.3445	5.7527	6.3291	7.3586	6.8001
ϕ=60	7.2356	6.4704	4.7931	6.0515	5.9695	6.8625	6.8856	5.7278
ϕ=70	6.9135	6.2165	4.6524	6.0038	6.3901	7.5136	6.5774	5.1493
ϕ=80	6.5658	5.9249	4.4773	6.1931	7.1623	8.5512	6.2801	4.7416
ϕ=90	6.1797	5.5836	4.2605	6.8894	8.5929	10.3594	6.0596	4.8667

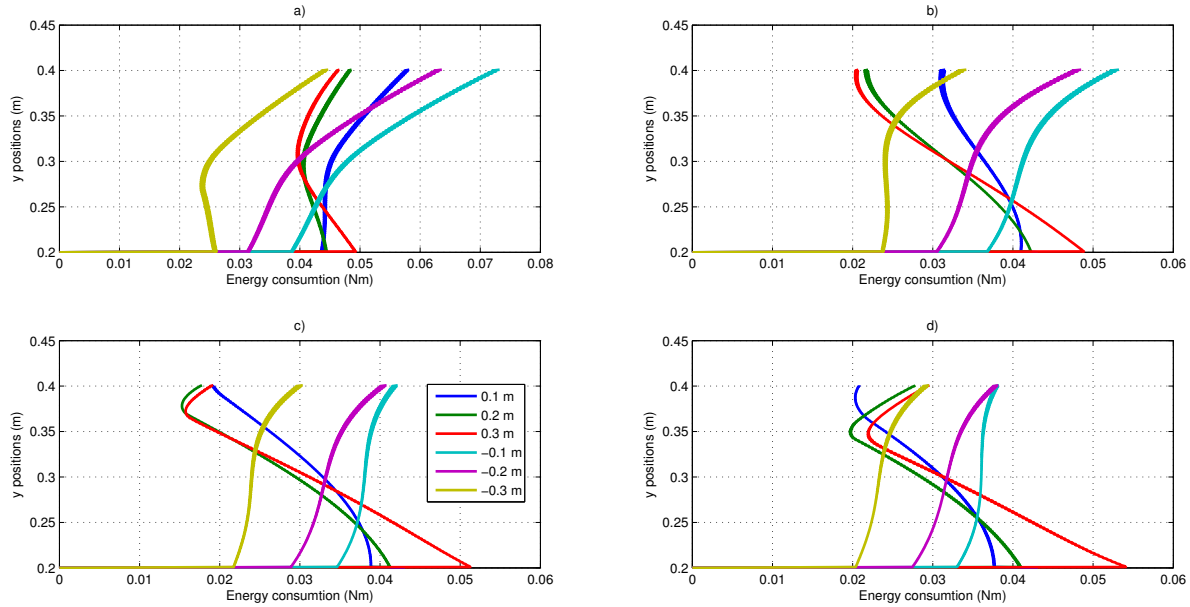

Figure 10 – Variation of the energy consumption with the y axis position of the (P)RRR+2RRR for: a) ϕ=0, b) ϕ=20, c) ϕ=45, d) ϕ=60

CONCLUSIONS

In this paper, three parallel planar manipulators, the *3RRR*, the *4RRR* and the *(P)RRR+2RRR*, are compared in terms of energy efficiency. Kinematic redundancy gets the best results in average, this can be due to the fact of its great reconfiguration possibilities. The orientation angle has been prove to play an important role in the energy efficiency for this kind of machines, for this reason, orientation angle can be treated as a variable to optimize. The actuation redundancy allows the systems to get a wide range of orientation angles, therefore *4RRR* has shown good energy performance at orientation angles from 45 to 90 degrees. Consequently, the addition of redundancy to the parallel planar manipulators achieves to improve their energy efficiency.

ACKNOWLEDGMENTS

This work is supported by the FP7-EMVeM (Energy efficiency Management for Vehicles and Machines) and FAPESP (2014/01809-0). Maíra M. da Silva is thankful for her Grant CNPq 02588/2011-6.

REFERENCES

Bi, Z. M., Wang, L., 2012, Energy Modeling of Machine Tools for Optimization of Machine Setups, IEEE Transactions on Automation Science and Engineering, Vol. 9, No. 3, July 2012.

Fontes, J. V., da Silva, M. M., 2014, Torque Optimization of Parallel Manipulators by the Application of Kinematic Redundancy, CONEM 2014.

Gosselin, C., Angeles, J., 1990 , Singularity Analysis of Closed-Loop Kinematic Chains, IEEE Transactions on Robotics and Automation.

Kim, J., Maranit, G., Chung, W. K. and Yuhl, J., 2004, A General Singularity Avoidance Framework for Robot Manipulators: Task Reconstruction Method, Proceedings of 2004 IEEE International International Conference on Robotics and Automation.

Kotlarski, J., Abdellatif, H., Heimann, B., 2008, Improving the pose accuracy of a planar 3RRR parallel manipulator using kinematic redundancy and optimized switching patterns, 2008 IEEE International Conference on Robotics and Automation, Pasadena, CA, USA, May 19-23, 2008.

Kotlarski, J., Abdellatif, H., Ortmaier, T. and Heimann, B., 2009, Enlarging the Useable Workspace of Planar Parallel Robots using Mechanisms of Variable Geometry, International Conference on Reconfigurable Mechanisms and Robots.

Li, Y. and Gary, M. B., 2001, Are Parallel Manipulators More Energy Efficient?, Proceedings of 2001 IEEE International Symposium on computational Intelligence in Robotics and Automation.

Mayorga, R. V. and Chandana, S., 2006, A NeuroFuzzy Approach for the Motion Planning of Redundant Manipulators, 2006 International Joint Conference on Neural Networks.

Pellicciari, M., Berselli, G., Leali, F. and Vergnano, A., 2013, A method for reducing the energy consumption of pick-and-place industrial robots, www.elsevier.com/locate/mechatronics

Wu, J., Wang, J., Wang, L., You, Z. 2010, Performance comparison of three planar 3-DOF parallel manipulators with 4-RRR , 3-RRR and 2-RRR structures, Mechatronics 2010, 20(4), pp. 510-517.

RESPONSIBILITY NOTICE

The author(s) is (are) the only responsible for the printed material included in this paper.